Journal of Structural Geology, Vol. 8, No. 6, pp. 597 to 605, 1986
Printed in Great Britain

0191-8141/86 $03.00 + 0.00
Pergamon Journals Ltd.

Experimental fracture, strain and subsidence patterns over en échelon strike–slip faults: implications for the structural evolution of pull-apart basins

MARK R. HEMPTON

Geology Research, Bellaire Research Center, Shell Development Company, Houston, TX 77001 U.S.A.

and

KURT NEHER

Department of Geology and Earth Sciences and Resources Institute, University of South Carolina, Columbia, SC 29208 U.S.A.

(*Received* 22 *March* 1985; *accepted in revised form* 10 *September* 1985)

Abstract—Claybox experiments show that with progressive left-lateral displacement on basal left-stepping, en échelon strike–slip faults an extremely complicated zone of evolving fracture, strain and subsidence patterns develops in the overlying clay. The fracture pattern is more complex than predicted by theoretical models and consists of a progressively widening array of Riedel shears, conjugate Riedel shears, and tension gashes above basal master faults. Conjugate Riedel shears rotate anticlockwise and lengthen, forming S-shaped fractures. Riedel shears rotate both anticlockwise and clockwise. Those that rotate anticlockwise eventually open as tension gashes. Other tension gashes open where the ends of Riedel and conjugate Riedel shears link. Strain contours in the deformed clay show an asymmetrical Z-shaped pattern over the stepover area between basal en échelon faults. In the early stages of displacement, strain is distributed penetratively over a progressively broadening zone. In later stages of displacement strain is partitioned into a narrow middle zone. Maximum strain is sustained always in the middle of the sheared zone and increases exponentially with progressive displacement. Subsidence is accommodated in the stepover area by oblique-slip on many Riedel and conjugate Riedel shears distributed throughout the stepover area. Subsidence (y) exhibits a linear relationship with master fault displacement (x) described by $y = 0.36x - 1.4$. The experimental fracture, strain and subsidence patterns in clay over en échelon faults can be used as interpretive and predictive tools with which to constrain interpretations of static field examples, especially in pull-apart basins on the crustal scale where many similarities with the models exist.

INTRODUCTION

FOR DISCONTINUOUS strike–slip faults that stepover in the same sense as displacement (e.g. right-stepping faults within a right-lateral fault system) there is growing interest in understanding how individual faults interact and evolve with progressive displacement (Ramsay 1980, Rodgers 1980, Segall & Pollard 1980, Bahat 1983). This is especially true on the crustal scale where progressive displacement on such discontinuous faults causes extension between the faults where their ends overlap (the stepover area) and results in a depression or pull-apart basin (Aydin & Nur 1982, Mann *et al.* 1983, Aydin & Page 1984). Specific questions concern: (1) the nature, orientation and distribution of secondary structures associated with displacement on primary master faults; (2) the nature of strain within and surrounding the stepover area and (3) the magnitude of subsidence in the stepover area.

This issue has been approached theoretically by Rodgers (1980), who used elastic dislocation theory, and Segall & Pollard (1980), who used the elastic interaction method. These models, although different in approach, have successfully accounted for the geometry of faults associated with some field examples. However, the results of Rodgers (1980) and Segall & Pollard (1980) are strictly valid only for the initial stages of displacement and not for finite deformations associated with many episodes of slip. Hence, their significance may be limited.

This study takes an experimental approach. We use a large clay box with basal plates defining en échelon discontinuous faults to study the development of faults, strain and subsidence in overlying clay which sustains progressive shear strain. The value of experimenting with clay has been emphasized by several workers (Hubbert 1937, H. Cloos 1939, E. Cloos 1955, Oertel 1965, Withjack & Scheiner 1982). This method has been successfully employed to study structures associated with pure strike–slip faults (Tchalenko 1970, Wilcox *et al.* 1973, Koide & Bhattacharji 1975) and pure extensional faults (E. Cloos 1955, Elmohandes 1981) but never used to examine the development of structures and strain associated with the stepover area between en échelon discontinuous strike–slip faults [except for a single crude run reported by Rodgers (1984)]. The purpose of this paper is to (1) describe and interpret fracture, strain and subsidence patterns produced in clay throughout successive stages of displacement; (2) compare these results with those of theoretical and field studies and (3) discuss the implications for the structural and extensional evolution of pull-apart basins.

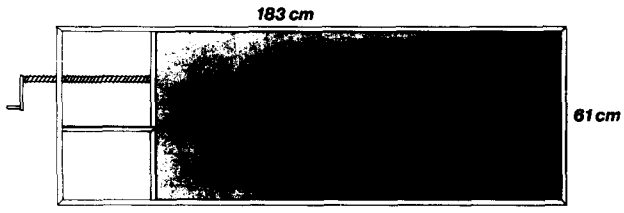

Fig. 1. Plan-view diagram of the experimental shear box. Basal plates are shaded gray. The box is 45 cm deep and clay fills gray areas to a depth of 15 cm. Thick black lines represent sawcuts separating basal plates. By cranking the bolt at left, the attached upper basal plate moves to the left creating a left-lateral shear system in the overlying clay and a gap in the 2.5 cm thick basal plates at the stepover.

EXPERIMENTAL AND OBSERVATIONAL METHODS

A shear box measuring 183 × 61 × 40 cm with 2.5 cm thick basal plates containing en échelon master faults characterized by a separation of 10 cm and an initial overlap of zero (constructed after the manner of Larter & Allison 1983) was used to generate 10 experimental runs in 15 cm thick Redart clay (Fig. 1). The clay contained 50% water by weight. At the start of each run the clay surface was smoothed and inscribed with circular markers. Left-lateral strike–slip displacement was driven by a hand-cranked bolt at an average rate of 4.2 × 10^{-3} cm s^{-1}. With progressive displacement in the stepover area between the basal-plate master faults, the overlying clay extended and subsided to form a depression. The magnitude of displacement equalled the amount of overlap between the master faults because the starting configuration represented an overlap of zero. Displacement was periodically halted to record displacement, time and depth of the depression; and to photograph the deformation features on the surface of the clay. To minimize boundary effects, the thickness of the clay was maintained a constant 15 cm by sheet-metal sides affixed to the basal plates. Only the clay overlying the stepover area was free to stretch and subside.

Ten experimental runs were conducted under the same conditions and they generated identical deformation features. We concentrated our analysis on a single run as characterized by the data presented in Table 1 and Figs. 2–8). This run consisted of 14 stages (Table 1). Deformation maps illustrating fracture patterns were traced from photographs of 5 stages of the run (stages 6, 8, 10, 12 and 14). Strain contour diagrams for these five runs were generated by calculating the quadratic strain ratio λ_1/λ_2 for each ellipse on the clay surface that had evolved from a circular marker (λ_1 and λ_2 refer to the quadratic elongation along the major and minor strain axes of each ellipse, respectively) (Figs. 2b & c). The quadratic strain ratio describes the amount of distortional strain on the clay surface at each ellipse (Ramsay & Huber 1983). The quadratic strain ratio is related to extension (e) and ellipticity (R):

$$\frac{\lambda_1}{\lambda_2} = \frac{(1 + e_1)^2}{(1 + e_2)^2} = R^2.$$

Table 1. Data generated from a single experimental run

Stage	Displacement (cm)	Time (s)	Displacement rate (cm s^{-1} × 10^{-3})	Depth of basin (cm)
1	0	0	—	0
2	2.0	477	4.2	0
3	3.1	716	4.6	0
4	4.1	960	4.1	0
5	5.1	1199	4.2	0.5
6	6.1	1435	4.2	0.75
7	7.1	1678	4.1	1.0
8	8.1	1916	4.2	1.5
9	10.1	2395	4.2	2.3
10	12.2	2874	4.4	3.0
11	14.2	3359	4.1	4.0
12	16.2	3836	4.2	4.5
13	18.3	4317	4.4	5.0
14	20.2	4794	4.2	6.0

EXPERIMENTAL RESULTS (TABLE 1)

Stage 6 *(displacement* = 6.1 *cm)*

To the left of the stepover area, fractures consist mostly of closely spaced, parallel, conjugate Riedel shears (Fig. 2a). They lengthen with progressive displacement. The newly formed ends form in the 70–80° conjugate Riedel orientation while their centers rotate anticlockwise. This produces a slightly sigmoidal configuration. Some short Riedel shears have formed and truncate conjugate Riedel shears. The stepover area is unfractured. To the right of the stepover area fractures consist of short Riedel and conjugate Riedel shears. Some Riedel shears cut conjugate Riedel shears although most shears are moving independently Some conjugate Riedel shears turn into the Riedel shear orientation at their ends.

Calculation of strain (Fig. 2b) shows that the strain pattern is asymmetric about the stepover area (Fig. 2c). Strain contours exhibit a Z-shaped pattern. Strain is greatest in the middle of the shear zone and grades towards the margins. There are three areas of highest strain within the middle of the shear zone where strain = 2.2 (Fig. 2c). Near the ends of the master faults the strain is relatively low. Subsidence in the stepover area has produced a depression 0.75 cm deep.

Stage 8 *(displacement* = 8.1 *cm)*

The zone of shearing has widened to about 40 cm. Conjugate Riedel shears are lengthened, more rotated, and form pronounced sigmoids (Fig. 3a). Some conjugate Riedel shears consist of shorter en échelon conjugate Riedel shears. Riedel shears have become more prominent. They have increased in length and truncate conjugate Riedel shears. Some very short, closely spaced and parallel Riedel shears form a narrow elongate zone oriented as a larger composite conjugate Riedel shear. The stepover area is surrounded by Riedel shears and conjugate Riedel shears. Both types of shear

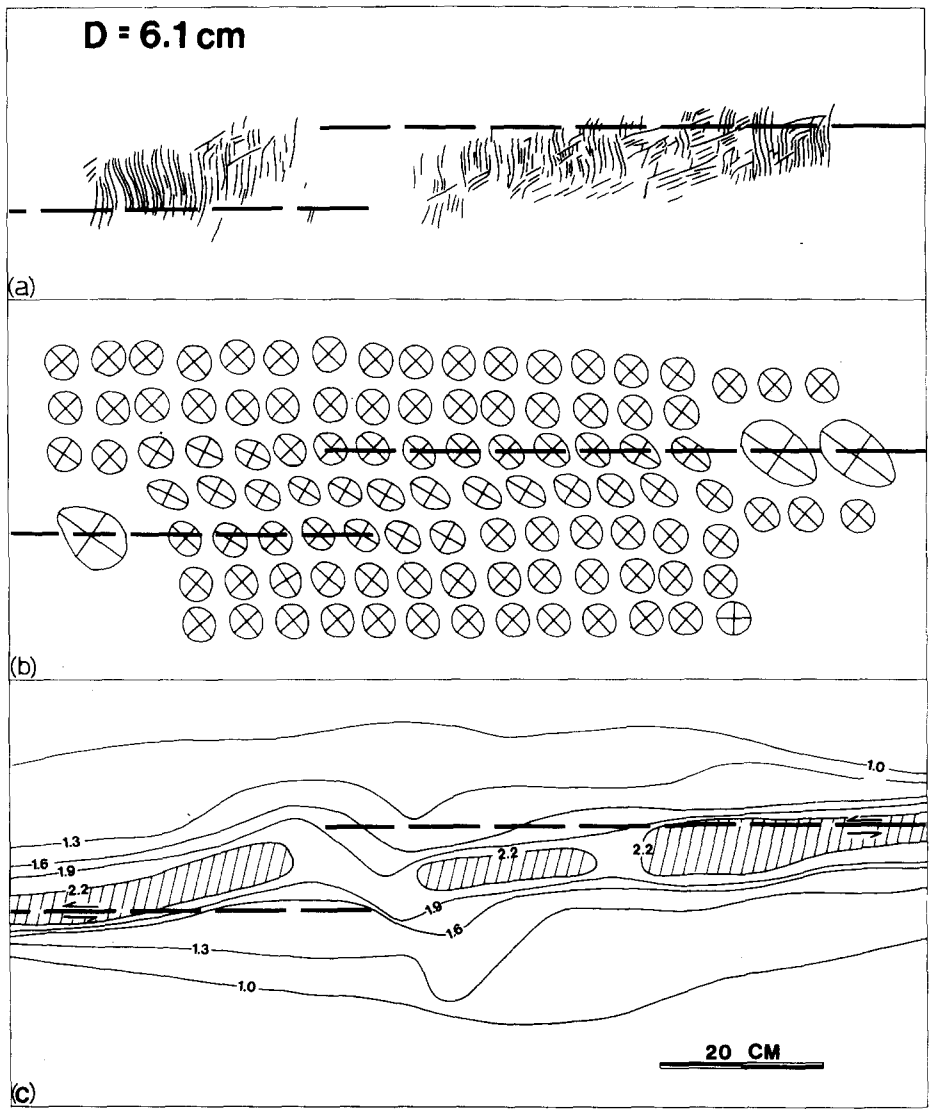

Fig. 2. Experimental results after displacement of 6.1 cm. Thick dashed lines represent position of underlying left-lateral strike-slip faults in basal plates. (a) Line drawing (traced from photograph) representing the fracture pattern consisting of Riedel shears, conjugate Riedel shears and slightly rotated conjugate Riedel shears. (b) Line drawing (traced from photograph) representing amount of strain sustained by clay. Similar line drawings are used to evaluate each stage illustrated in Figs. 3–6. (c) Contours of strain values calculated from each ellipse in (b). Hatched areas represent zones of maximum strain. Maximum subsidence is measured in the center of the stepover area and equals 0.75 cm.

in the stepover area are characterized by oblique-slip which has allowed the depression to subside to 1.5 cm.

The zone of strain contours has widened and an asymmetric Z-shaped pattern of strain contours has formed around the stepover area (note especially the 1.4 contour); (Fig. 3b). There are three areas of highest strain within the center of the shear zone where strain = 3.0 (Fig. 3b). Strain at the ends of the master faults is higher than that in the area along the master faults about 10 cm away from the ends.

Stage 10 *(displacement* = 12.2 *cm)*

By this stage Riedel and conjugate Riedel shears have become more numerous and longer to form a complicated intersecting network (Fig. 4a). Conjugate Riedel shears are still predominant to the left of the stepover area. Some short closely spaced conjugate Riedel shears are aligned parallel to one another to form a composite narrow zone in the Riedel orientation. In the center of the deformed zone, conjugate Riedel shears have rotated anticlockwise to 110–120° from the horizontal while those near the margin are forming at 75–80°. Rotated conjugate Riedel shears in the center are linking with both marginal conjugate Riedel shears and Riedel shears to produce growing S-shaped fracture trends. Elongating Riedel shears dominate to the right of the stepover area. In all cases, they truncate pre-existing conjugate Riedel shears. Long segments of elongate Riedel shears are rotated clockwise and resemble the elongate Riedel shears on the floor of the Rhine graben (Illies 1981). Other smaller segments of Riedel shears have rotated anticlockwise. Some of these segments have rotated so much that they assume the tension gash orientation and open as small holes. Other small holes open where Riedels and conjugate Riedel shears are linked. Some short closely spaced Riedel shears are aligned parallel to form composite narrow zones in the

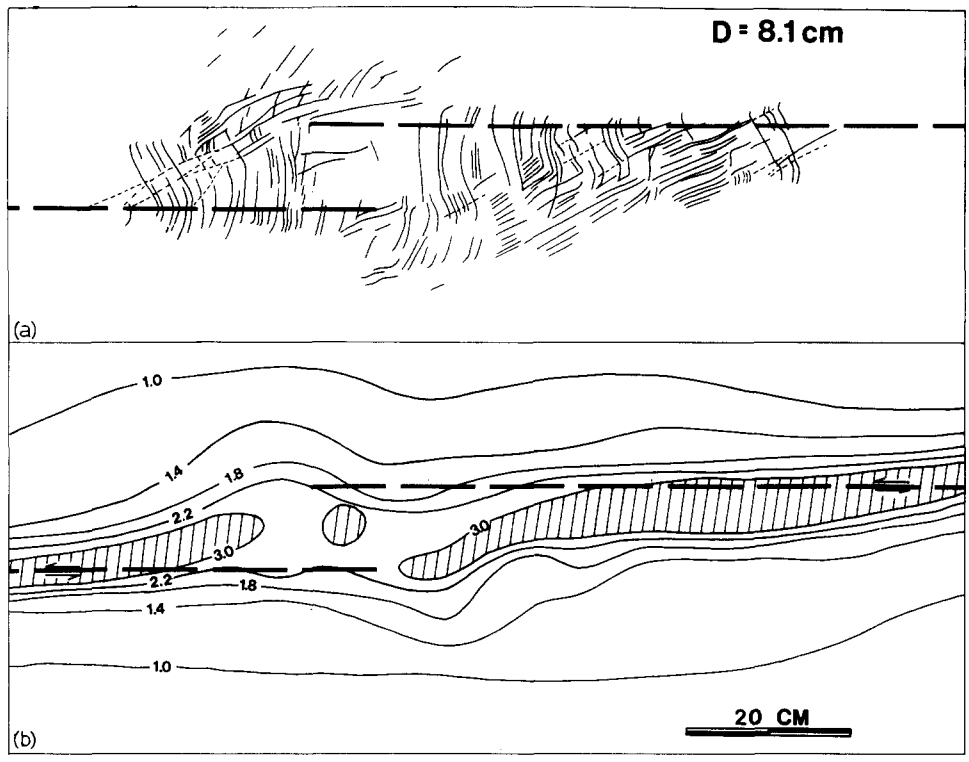

Fig. 3. Experimental results after displacement of 8.1 cm. See Fig. 2 for a description of the symbols and methodology. (a) Line drawing (traced from photograph) representing the fracture pattern. (b) Contours of strain calculated in the same manner as in Fig. 2. Maximum subsidence is 1.5 cm.

conjugate Riedel orientation. A large portion of the stepover area remains unaffected by fractures. This area has subsided 3.0 cm.

The strain pattern remains asymmetric but has grown wider (Fig. 4b). Strain in the middle of the shear zone is greater (S = 5.0) and the three areas of greatest strain persist. As in the two previous stages, the closely spaced strain contours curve into the stepover area near the ends of the master faults isolating two relatively low-strain areas within high-strain areas. Compared with the previous stages, these low-strain areas are becoming more pronounced and are moving towards each other.

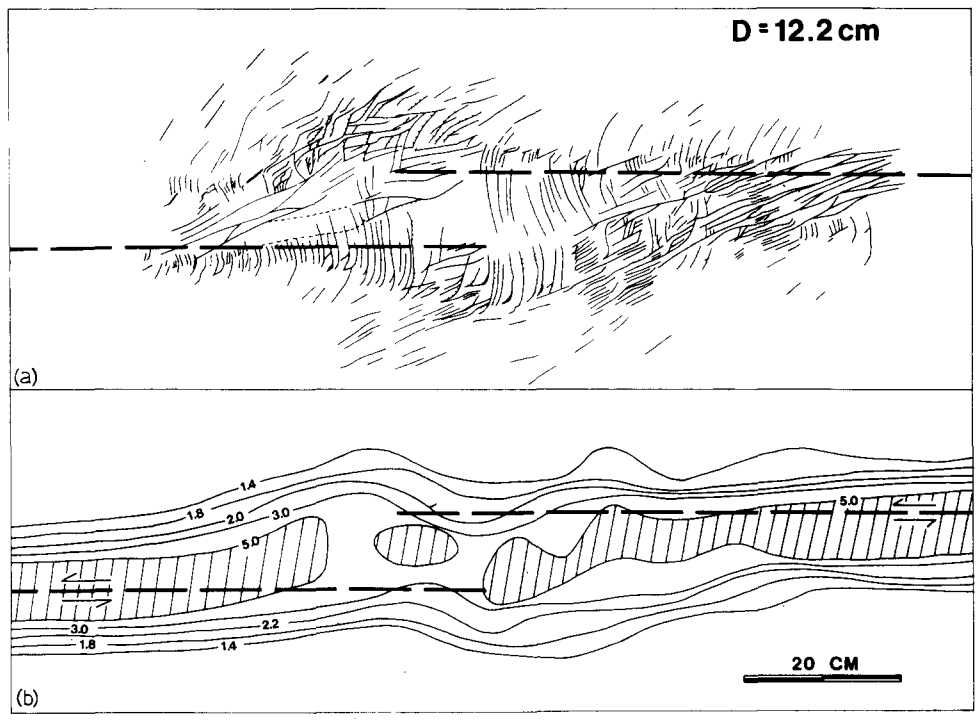

Fig. 4. Experimental results after displacement of 12.2 cm. See Fig. 2 for a description of the symbols and methodology. (a) Line drawing (traced from photograph) representing the fracture pattern. Fractures with ticks on one side represent normal–slip. (b) Contours of strain calculated in the same manner as in Fig. 2. Maximum subsidence is 3.0 cm.

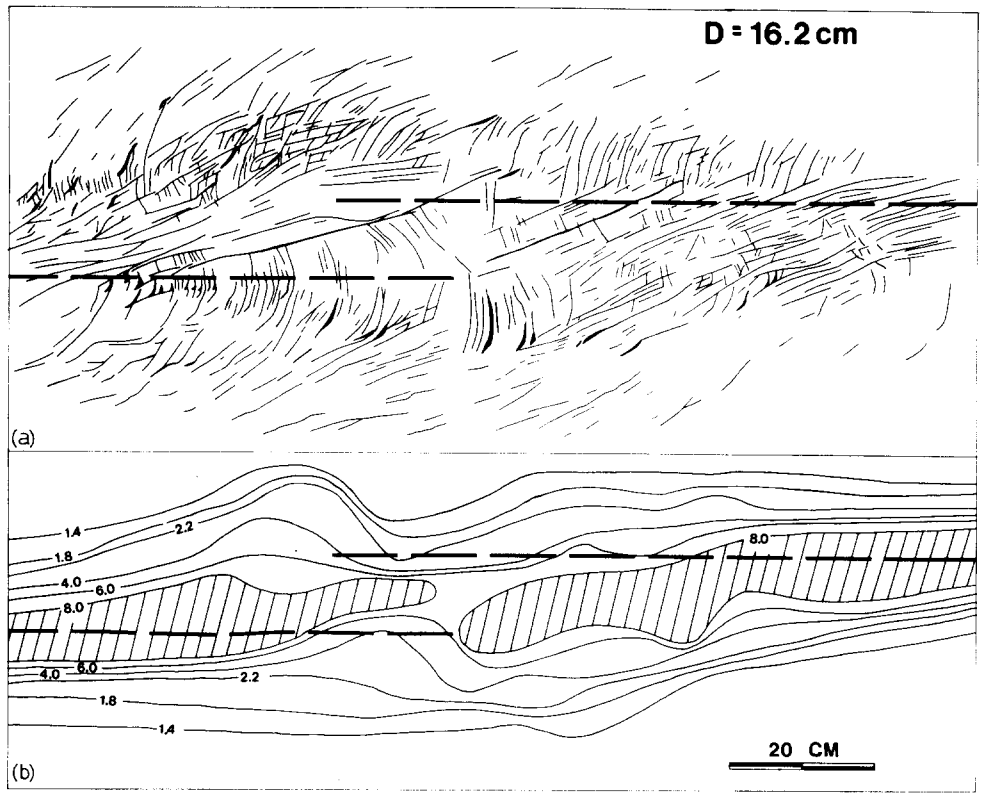

Fig. 5. Experimental results after displacement of 16.2 cm. See Fig. 2 for a description of symbols and methodology. (a) Line drawing (traced from photograph) representing the fracture pattern. (b) Contours of strain calculated in the same manner as in Fig. 2. Maximum subsidence = 4.5 cm.

Stage 12 *(displacement* = 16.2 *cm)*

At this stage of displacement many Riedel shears are developed at the margins of the shear zone resulting in a wider swath of deformation (Fig. 5a). Riedel shears are more numerous and truncate conjugate Riedel shears producing large areas of intersecting shears that are well-developed in the northwest and southeast quadrants. Many Riedel shears have grown longer, particularly those near the stepover area. Segments of many conjugate Riedel fractures have also elongated and rotated anticlockwise, resulting in an even more pronounced S-shaped configuration. The surface of the stepover area is much less deformed, although it has subsided to 4.5 cm. Small folds oriented at 130–135° to the horizontal have developed on the top of the subsiding surface (Fig. 5a).

Strain contours form a wider pattern that is asymmetric, although less so than in previous stages (Fig. 5b). The magnitude of maximum strain has increased to S = 8. Within the middle of the shear zone there are now just two areas of highest strain separated by an area of lower strain within the stepover area. The low-strain areas surrounded by high-strain areas near the ends of the master faults have moved closer to one another across the stepover area.

Stage 14 *(displacement* = 20.2 *cm)*

The most striking aspects of this stage are (1) the densely spaced character of new Riedel and conjugate Riedel shears, (2) the densest concentration of Riedel and conjugate Riedel shears forms an elongate zone parallel to the master faults and curving around the stepover area and (3) the number and size of extensional openings (Fig. 6a). Riedel shears near the master faults have elongated and assumed a curvilinear configuration. Many new conjugate Riedel shears have developed between long parallel Riedel shears. Long segments of the elongate Riedel shears have rotated clockwise towards the orientation of the master faults. The extensional openings form in two different environments where (1) Riedel shears link with conjugate Riedel shears and (2) short segments of long Riedel shears have rotated anticlockwise into the tension gash orientation. Once these openings form, much of the strain within the shear zone is accommodated by their continued opening rather than by movement on Riedel and conjugate Riedel shears. The surface of the stepover area remains relatively unsheared although it is undergoing compression as it subsides. By this stage of displacement it has subsided to 6.0 cm.

The strain contours show a slightly asymmetric configuration around the stepover area (Fig. 6b). Strain within the middle of the shear zone has increased markedly to S = 25. There are three areas of maximum strain. The middle maximum strain area is centered over the stepover area. The low strain zones within the stepover area surrounded by high strain areas near the ends of the underlying master faults have moved closer. The ends of the master faults underlie areas of high strain gradient.

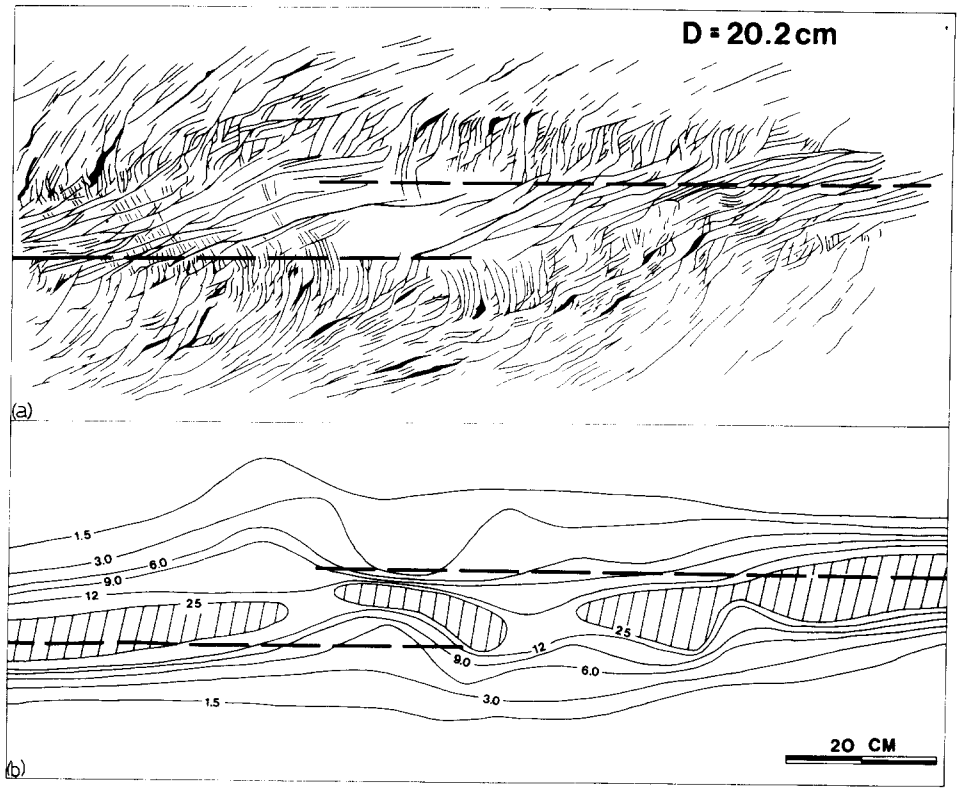

Fig. 6. Experimental results after displacement of 20.2 cm. See Fig. 2 for a description of symbols and methodology. (a) Line drawing (traced from photograph) representing the fracture pattern. (b) Contours of strain calculated in the same manner as in Fig. 2. Hatched areas represent zones of maximum strain. Maximum subsidence measured in the center of the stepover area is 6.0 cm.

DISCUSSION AND CONCLUSIONS

Fracture pattern

The evolution of the fracture pattern in the clay overlying en échelon basal master faults is not as simple as predicted by theoretical models or observed in experiments in clay involving a single straight, basal strike–slip fault. The zone of fractures in the clay grows wider and more complicated with progressive displacement. Most of the shear displacement is accommodated in the middle of the deformed zone and dissipates outwards. The first shears to form are conjugate Riedel shears and they are soon cut by Riedel shears. Riedel shears and conjugate Riedel shears become more numerous with progressive displacement, although Riedel shears predominate in the later stages. As displacement progresses, conjugate Riedel shears elongate and their center segments are rotated anticlockwise. This produces a marked sigmoidal configuration. Riedel shears elongate and portions are rotated both clockwise and anticlockwise. Only short portions rotate anticlockwise. When these short portions rotate into an orientation parallel to the maximum compressive stress, the Riedel shears open as tension gashes. Other openings form in similar orientations where the ends of conjugate Riedel shears link with the ends of Riedel shears. The stepover area remains relatively undeformed until cut by throughgoing elongate Riedel shears at D = 16.2 cm. The orientation of these Riedel shears corresponds to the orientation of the stepover shear proposed theoretically by Rodgers (1980) for the surface expression of buried master faults (his fig. 6b). The orientation of the stepover Riedels also corresponds to the orientation of "secondary shear fractures near en échelon discontinuities" according to the theoretical modelling of Segall & Pollard (1980). Riedel shears and conjugate Riedel shears for the most part intersect and form complex fault-block domains. The most closely spaced zones of intersecting shears form over the ends of the basal master faults. Although experimental studies of clay overlying single straight master faults delineated *P* shears and 'principal displacement shears' (which formed parallel to the underlying master fault) (Tchalenko 1970, Wilcox *et al.* 1973) no such structures form in clay over en échelon faults after displacement of 20.2 cm.

The significance of the experimental fracture pattern lies in the fact that an initially isotropic material such as clay develops such a complicated fracture pattern involving complex and evolving interactions between numerous, densely distributed Riedel shears, conjugate Riedel shears and tension gashes in the accommodation of shear displacement over the stepover area between two basal master faults. This should help us appreciate the structural complexity developed in analogous natural environments involving alluvium over en échelon basement faults or within pull-apart basins. The evolving fracture pattern involving rotating Riedel shears, conjugate Riedel shears, and tension gashes shows that the standard Riedel experimental fracture template so often

referred to in the literature (e.g. Reading 1980) cannot be applied to every stage of displacement along every shear zone. Riedel shears, conjugate Riedel shears, and tension gashes all rotate with progressive displacement.

The experimental evolution of structures can provide a basis from which to understand the complex evolution of structures within heterogeneous assemblages of basement rocks near the stepover area of two crustal-scale en échelon faults defining a pull-apart basin. We know that the homogeneous clay reflects perhaps the ideal fracture pattern for the particular strain rate and depth of clay in the experiment. This fracture pattern is exceedingly complex. In the earth's crust with different rock types and pre-existing structures we can expect an even more complicated fracture pattern, though aware of an ideal pattern produced experimentally in the clay. This proposal assumes greater significance in light of the increasingly more common recognition of strike–slip faults moving over mid-crustal horizontal detachment surfaces (Royden *et al.* 1983, Sibson 1983). The broad anastomosing fracture pattern produced in the experiments is very similar to the wide and diffuse fault pattern surrounding well-mapped pull-apart basins (Mann *et al.* 1983). A particularly good example is the fault pattern in the Gulf of Elat (Ben-Avraham 1985). The experimental fracture patterns may be used to predict and interpret structures in continental areas where pull-apart basins are known to have initiated, for example, Belize in the Caribbean which was affected by the developing Cayman Trough pull-apart system (Mann *et al.* 1983).

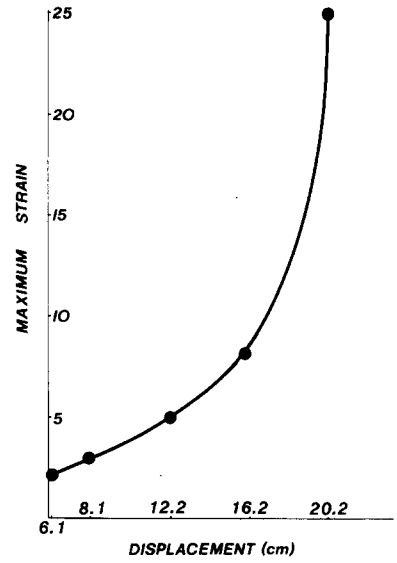

Fig. 7. Graph showing how maximum strain (λ_1/λ_2) increases with increasing displacement for a single experimental run. Filled circles represent values of maximum strain and displacement associated with the stages of the experimental run illustrated in Figs. 2–6.

Strain pattern

The strain contour pattern broadens with progressive displacement. A prominent Z-shaped configuration of contours develops over the stepover area and is maintained throughout successive displacements. The reasons for this pattern are uncertain, but must be related to the manner in which shear strain is transferred between master faults in the stepover area. The ends of the master faults lie under relatively high-strain areas while areas over the basal master faults about 10 cm from the ends exhibit low strain. These low-strain areas migrate toward each other with progressive displacement along the master faults. By Stage 14, displacement is 20.2 cm and the low-strain areas are nearly adjacent to each other. With greater displacement, this pattern predicts that the low-strain areas will merge and separate the central area of highest strain. In other words, two areas of high strain separated by an area of low strain develop in the stepover area. This observation may help to explain Rodger's (1980) proposal that when overlap of the en échelon master faults is twice the separation in pull-apart basins, the two sub-basins develop between the ends of the two faults within a larger basin. In Fig. 6(b) the overlap is nearly twice the separation of the master faults and the low-strain areas are merging to divide the high strain area into two separate domains (depressions) near the ends of the master faults. High-strain areas follow the ends of the master faults. When overlap is twice as much as separation, a single high-strain area is split by merging low-strain zones. On the crustal scale, several pull-apart basins are known to contain two sub-basins near the ends of master faults, for example, Cariaco Basin, offshore Venezuela (Schubert 1982) and the Dakar, Aragonese and Elat Basins in the Gulf of Elat (Ben-Avraham *et al.* 1979, Ben-Avraham 1985).

Maximum strain is sustained in the middle of the shear zone (Figs. 2–6). A plot of maximum strain versus displacement for the stages illustrated in Figs. 2–6 is shown in Fig. 7. Maximum strain increases slowly at first, (until D = 16.2 cm) probably because shear strain is accommodated over a broad zone. After D = 16.2 cm, maximum strain increases rapidly. This indicates that more shear strain per cm of displacement is accommodated in the middle of the deformation zone relative to the previous stages. The partitioning of proportionally greater quantities of shear strain into the middle of the deformation zone happens even though the zone as a whole is growing wider. The early distribution of small values of strain over a broad area followed by later concentration of large amounts of strain into a narrow zone is a pattern recognized in many field examples of pull-apart basins (Mann *et al.* 1983). The later phases of strain concentration in a narrow middle zone is probably the greatest contributing factor to the death of pull-apart basins. Their sediments are compressed and uplifted as the original en échelon master faults are superseded by a single straight strike–slip fault.

Subsidence pattern

With progressive displacement on the master faults the stepover area subsides by oblique–slip on many, densely distributed Riedel and conjugate Riedel frac-

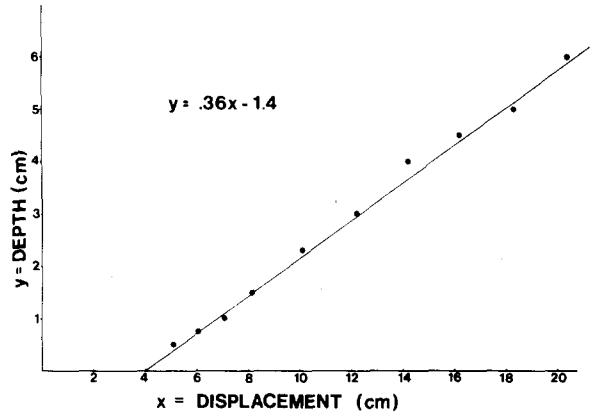

Fig. 8. Graph showing how depth (y) of the stepover area increases linearly with increasing displacement (x) according to the equation $y = 0.36x - 1.4$. Filled circles represent values of depth and displacement for each stage of the experimental run indicated in Table 1.

tures. Figure 8 shows a linear relationship between subsidence and displacement expressed as the equation $y = 0.36x - 1.4$ where y = subsidence and x = displacement. The positive x intercept shows that subsidence does not commence until a small amount of displacement, probably because of the cohesive character of the clay. The linear nature of this experimentally derived relationship is similar to the linear nature of the empirical relationship between strike–slip displacement and sediment thickness in pull-apart basins derived by Hempton & Dunne (1984). Hence, the experimental relationship supports the contention of Hempton & Dunne (1984) that subsidence in pull-apart basins depends on the amount of crustal stretching which in turn is a function of strike–slip displacement on master faults.

Significance and limitations of the experiment

We qualify our experimental results by recognizing the inherent limitations of the experiment. Even though Hubbert (1937) suggested that wet clay could be used in the scale modelling of natural structural phenomena, we realize that in our experiment, boundary conditions are not completely eradicated (despite the large clay box). Furthermore, we have introduced an unnatural vertical effect by using basal plates of a constant thickness. It is difficult (and probably impossible) to accurately model the subsidence of stretched and thinned lithosphere. However, in the manner of E. Cloos (1955), we propose that even with the experimental limitations the results are very significant for helping us to understand similar phenomena in nature.

Many features associated with natural en échelon strike–slip faults (particularly those on the crustal scale defining pull-apart basins) are replicated in the controlled setting of the experiment and support interpretations of field examples. The experiments generated similar fracture types and patterns; evidence that high-strain areas are located near the ends of master faults and can be separated by low-strain areas; and amounts of subsidence between en échelon faults that are linearly related to amounts of displacement. The experiments are valuable because they have exhibited features not observable in the field. For example, we have been able to quantify and contour strain around the stepover area. The experiments have allowed us to study the evolution of fracture, strain and subsidence patterns with progressive amounts of displacement. These patterns can be used as interpretive and predictive tools with which to understand better static field examples.

Acknowledgements—We conducted these experiments as members of the Geology Department at Carleton College. We thank Tim Vick, technical director, for his assistance in all phases of the experiments. Much of this work is built upon preliminary studies of en échelon faults in clay by David Gallo and Rob Alexander. We thank Paul Mann, Jeff Fox, Dwight Bradley, A. M. C. Şengör, Lorie Dunne, Mark Gordon, John Dewey and Kevin Burke for many stimulating discussions.

REFERENCES

Aydin, A. & Nur, A. 1982. Evolution of pull-apart basins and their scale independence. *Tectonics* **1**, 91–105.

Aydin, A. & Page, B. M. 1984. Diverse Pliocene–Quaternary tectonics in a transform environment, San Francisco Bay region, California. *Bull. geol. Soc. Am.* **95**, 1303–1317.

Bahat, D. 1983. New aspects of rhomb structures. *J. Struct. Geol.* **5**, 591–601.

Ben-Avraham, Z. 1985. Structural framework of the Gulf of Elat (Aqaba), Northern Red Sea. *J. geophys Res.* **90**, 703–726.

Ben-Avraham, Z., Almagor, G. & Garfunkel, Z. 1979. Sediments and structure of the Gulf of Elat. *Sediment. Geol.* **23**, 239–267.

Cloos, E. 1955. Experimental analysis of fracture patterns. *Bull. geol. Soc. Am.* **66**, 241–256.

Cloos, H. 1939. Hebung, Spaltung, Vulkanismus. *Geol. Rdsch.* **30**, 405–527.

Elmohandes, S. 1981. The central European graben system: rifting imitated by clay modelling. *Tectonophysics* **73**, 69–78.

Hempton, M. R. & Dunne, L. A. 1984. Sedimentation in pull-apart basins: active examples in eastern Turkey. *J. Geol.* **92**, 513–530.

Hubbert, M. K. 1937. Theory of scale models as applied to the study of geologic structures. *Bull. geol. Soc. Am.* **48**, 1459–1521.

Illies, J. H. 1981. Mechanism of graben formation. *Tectonophysics* **73**, 249–266.

Koide, H. & Bhattacharji, S. 1975. Geometric patterns of active strike–slip faults and their significance as indicators for areas of energy release. In: *Energetics of Geological Processes* (edited by Saxena, S. K. & Bhattacharji, S.). Springer, New York, 47–66.

Larter, R. C. L. & Allison, I. 1983. An inexpensive device for modelling strike–slip and oblique–slip fault zones. *J. Geol. Ed.* **31**, 200–205.

Mann, P., Hempton, M. R., Bradley, D. C. & Burke, K. 1983. Development of pull-apart basins. *J. Geol.* **91**, 529–554.

Oertel, G. 1965. The mechanism of faulting in clay experiments. *Tectonophysics* **2**, 343–393.

Ramsay, J. G. 1980. Shear zone geometry: a review. *J. Struct. Geol.* **2**, 83–99.

Ramsay, J. G. & Huber, M. I. 1983. *The Techniques of Modern Structural Geology, Volume* 1. Academic Press, London.

Reading, H. G. 1980. Characteristics and recognition of strike–slip systems. In: *Sedimentation in Oblique–Slip Mobile Zones* (edited by Ballance, P. F. & Reading, H. G.). International Association of Sedimentologists. Oxford, 7–26.

Rodgers, D. A. 1980. Analysis of basin development produced by en échelon strike–slip faults. In: *Sedimentation in Oblique–Slip Mobile Zones* (edited by Ballance, P. F. & Reading, H. G.). International Association of Sedimentologists. Oxford, 27–42.

Rodgers, D. A. 1984. Mexia and Talco fault zones, East Texas: comparisons of origins predicted by two tectonic models. In: *The Jurassic of East Texas* (edited by Presley, M. W.). East Texas Geological Society, 23–31.

Royden, L., Horvath, F. & Rumpler, J. 1983. Evolution of the Pannonian Basin system—I. Tectonics. *Tectonics* **2**, 63–90.

Schubert, C. 1982. Origin of Cariaco basin, southern Caribbean Sea. *Marine Geol.* **47**, 345–360.

Segall, P. & Pollard, D. D. 1980. Mechanics of discontinuous faults. *J. geophys. Res.* **85**, 4337–4350.

Sibson, R. H. 1983. Continental fault structure and the shallow earthquake source. *J. geol. Soc. Lond.* **140**, 741–767.

Tchalenko, J. S. 1970. Similarities between shear zones of different magnitudes. *Bull. geol. Soc. Am.* **81**, 1625–1640.

Wilcox, R. E., Harding, T. P. & Seeley, D. R. 1973. Basic wrench tectonics. *Bull. Am. Ass. Petrol. Geol.* **57**, 74–96.

Withjack, M. O. & Scheiner, C. 1982. Fault patterns associated with domes—an experimental and analytical study. *Bull. Am. Ass. Petrol. Geol.* **66**, 302–316.